# REPORT DOCUMENTATION PAGE

*Form Approved*
*OPM No. 0704-0188*



| 1. AGENCY USE ONLY *(Leave blank)* | 2. REPORT DATE | 3. REPORT TYPE AND DATES COVERED |
|---|---|---|
| | July 1996 | Transmittal document |

**4. TITLE AND SUBTITLE**
Inverse Scattering Methods for Reconstructing Fluids

**5. FUNDING NUMBERS**
N00014-94-1-0286

**6. AUTHOR(S)**
Daniel Rouseff

**7. PERFORMING ORGANIZATION NAME(S) AND ADDRESS(ES)**
Applied Physics Laboratory
University of Washington
1013 NE 40th Street
Seattle, WA 98105-6698

**8. PERFORMING ORGANIZATION REPORT NUMBER**

**9. SPONSORING / MONITORING AGENCY NAME(S) AND ADDRESS(ES)**
Defense Technical Information Center
8725 John J. Kingman Road
Suite 0944
Ft. Belvoir, VA 22060-6218

**10. SPONSORING / MONITORING AGENCY REPORT NUMBER**



**11. SUPPLEMENTARY NOTES**
Reprint of paper submitted to fulfill grant obligation.

**12a. DISTRIBUTION / AVAILABILITY STATEMENT**
Unlimited.

**12b. DISTRIBUTION CODE**

**13. ABSTRACT** *(Maximum 200 words)*

The reconstruction of a two-dimensional moving fluid from acoustic transmission measurements is considered. The fluid is described by both a scalar index of refraction and a vector velocity. If the measured data are assumed to be straight-ray geometric projections of the flow, it is known that inversion for the vector velocity is an underdetermined problem. In the present work, it is shown that if the measured data are assumed to satisfy a linearized time-harmonic wave equation, then a unique inversion for the vector velocity is possible. This result is a distinctly finite wavelength effect indicating why ray-based methods fail to produce a complete reconstruction. A filtered backpropagation algorithm for the tomographic reconstruction of the vector flow field is derived.

| 14. SUBJECT TERMS | 15. NUMBER OF PAGES |
|---|---|
| Tomography, flow inversion, vector reconstruction, diffraction | 11 |
| | 16. PRICE CODE |

| 17. SECURITY CLASSIFICATION OF REPORT | 18. SECURITY CLASSIFICATION OF THIS PAGE | 19. SECURITY CLASSIFICATION OF ABSTRACT | 20. LIMITATION OF ABSTRACT |
|---|---|---|---|
| Unclassified | Unclassified | Unclassified | SAR |

Inverse Problems 10 (1994) 687–697. Printed in the UK

# Two-dimensional vector flow inversion by diffraction tomography

Daniel Rouseff and Kraig B Winters†

Applied Physics Laboratory, College of Ocean and Fishery Sciences, University of Washington, Seattle, WA 98105, USA

Received 17 November 1993

**Abstract.** The reconstruction of a two-dimensional moving fluid from acoustic transmission measurements is considered. The fluid is described by both a scalar index of refraction and a vector velocity. If the measured data are assumed to be straight-ray geometric projections of the flow, it is known that inversion for the vector velocity is an underdetermined problem. In the present work, it is shown that if the measured data are assumed to satisfy a linearized time-harmonic wave equation, then a unique inversion for the vector velocity is possible. This result is a distinctly finite wavelength effect indicating why ray-based methods fail to produce a complete reconstruction. A filtered backpropagation algorithm for the tomographic reconstruction of the vector flow field is derived.

## 1. Introduction

Consider an acoustic wave probing a moving fluid. In general, both the scalar index of refraction and the vector velocity describing the flow will be spatially varying with both fields affecting the transmitted acoustic wave. Assume the flow can be probed from many different directions. The inverse problem is to process the measured acoustic data to recover both the index of refraction and the velocity of the intervening fluid. Non-intrusive, tomographic flow inversion has a variety of practical applications including biomedical imaging, industrial or laboratory process monitoring and measuring ocean turbulence.

Flow inversion requires the reconstruction of both scalar and vector fields. Compared to scalar inversion, relatively little research has been done on vector reconstruction. An early study of flow imaging was conducted by Johnson *et al* [1]. They measured the acoustic time-of-flight between transmitting and receiving arrays. Neglecting refraction and diffraction, the data were assumed to be straight-ray, geometric projections of the flow along the transmission paths. Averaging the time-of-flight measurements from opposing directions approximately cancelled the effects of fluid motion. The scalar index of refraction was then reconstructed using standard techniques. Taking the difference between opposing measurements yielded projections of that component of flow velocity tangential to the direction of transmission. Efforts to reconstruct the flow velocity, however, meet with limited success. Norton [2] later showed that only the divergence-free (solenoidal) component of a two-dimensional vector field could be recovered from tomographic experiments. Consequently, full velocity inversion is underdetermined if a straight-ray forward model is assumed. Winters and Rouseff [3] showed that the transverse component of fluid vorticity could be recovered and derived a spatial domain inversion

† Also with Department of Applied Mathematics.

0266-5611/94/030687+11$19.50 

algorithm. A discrete version of this algorithm was tested on simulated flow fields typical of turbulent mixing in the upper ocean thermocline [4].

In each of the cited references, a straight-ray model was used for the forward problem. Clearly, this is an approximation. In a more accurate approach, an acoustic wave would be modelled by an acoustic wave equation. A tomographic method that uses a wave equation in the forward model is called diffraction tomography [5]. In the present work, we show that a two-dimensional vector flow field can be reconstructed using diffraction tomography. Thus an inverse problem that is apparently underdetermined using a simple forward model can be solved using a more accurate forward model. A filtered backpropagation algorithm for the vector velocity is derived. The vector inversion algorithm is shown to differ in several ways from the scalar inversion procedure derived by Devaney [6].

## 2. Diffraction tomography for flow inversion

Consider the propagation of sound through a two-dimensional moving fluid. The fluid is characterized by a scalar index of refraction $n(\boldsymbol{r})$ and a velocity vector $\boldsymbol{u} = (u, v)$. Here $\boldsymbol{r} = (x, y)$ is the spatial position vector and $\boldsymbol{u}(\boldsymbol{r})$ is scaled by the reference sound speed $C_0$. As a forward scattering model, the total time-harmonic $\exp(-i\omega t)$ acoustic pressure $p_t$ is assumed to satisfy

$$[\nabla^2 + k^2]p_t(\boldsymbol{r}) = -k^2 F(\boldsymbol{r})p_t(\boldsymbol{r}) - 2ik\boldsymbol{u}(\boldsymbol{r}) \cdot \nabla p_t(\boldsymbol{r}) \tag{1}$$

where $F(\boldsymbol{r}) = [n^2(\boldsymbol{r}) - 1]$ is the scattering function and $k = \omega/C_0$ is the reference wavenumber. This expression can be derived via a perturbation analysis from the conservation of momentum and the conservation of mass relationships [7]. Equation (1) neglects non-linear terms involving the flow velocity. A similar starting point was used by Norton in a study of transient scattering by stratified fluids [8]. The total pressure can be decomposed into the sum of the known incident field $p_i$ ensonifying the medium and the resulting scattered field $p$. The integral solution to (1) is

$$p_t = p_i + p \tag{2}$$

where

$$p(\boldsymbol{r}) = \frac{i}{4}\int_V d\boldsymbol{r}' [k^2 F(\boldsymbol{r}')p_t(\boldsymbol{r}') + 2ik\boldsymbol{u}(\boldsymbol{r}') \cdot \nabla' p_t(\boldsymbol{r}')]H_0^{(1)}(k|\boldsymbol{r} - \boldsymbol{r}'|) \tag{3}$$

and where $H_0^{(1)}$ is the Hankel function of the first kind and order zero. The integration is over the scattering domain.

Assume the scattering geometry shown in figure 1. The incident field is a unit amplitude plane wave propagating in the direction of the unit vector $\hat{\eta}$. The acoustic pressure is measured along a linear receiving array at $\eta = L$ where the scattering domain is confined to a circular region of radius less than $L$. The mean flow velocity taken over the scattering domain is assumed to be zero. Denote the measured scattered field as $p_\phi(\xi)$ where the subscript shows the explicit dependence of the measurement on the view direction $\phi$. For weak scattering, (3) can be linearized by making the Born approximation [9] and the unknown total field in the integrand replaced by the known incident field. The resulting measured scattered field is

$$p_\phi(\xi) = \frac{ik^2}{4}\int_V d\boldsymbol{r}' [F(\boldsymbol{r}') - 2\hat{\eta} \cdot \boldsymbol{u}(\boldsymbol{r}')]e^{ik\eta'}H_0^{(1)}(kR) \tag{4}$$

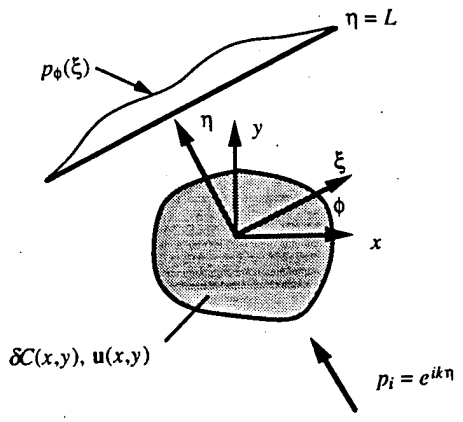


**Figure 1.** Schematic of acoustic transmission experiment. Incident plane wave $p_i$ probes moving fluid characterized scalar sound speed perturbation $\delta C$ and vector velocity $\boldsymbol{u}$. The coordinate system $(\xi, \eta)$ is defined by the probing direction $\phi$. Coherent scattered field $p_\phi(\xi)$ measured at $\eta = L$.

where $R^2 = (\xi - \xi')^2 + (L - \eta')^2$ and the integration is with respect to the fixed (unrotated) coordinates $r' = (x', y')$.

We assume the fluid can be probed from a continuum of view directions $\phi \in [0, 2\pi)$. The objective is to use this data set and the assumed forward scattering model (4) to recover the scattering potential $F$ and both components of the vector velocity $\boldsymbol{u}$. The relationship between the measured pressure and the unknowns can be expressed more simply in the Fourier domain. Define the one- and two-dimensional transforms

$$\begin{aligned} \tilde{p}_\phi(\kappa) &= \int_{-\infty}^{\infty} p_\phi(\xi) e^{-i\kappa\xi}\, d\xi \\ \tilde{F}(k_x, k_y) &= \int_{-\infty}^{\infty}\int_{-\infty}^{\infty} F(x, y) e^{-i(k_x x + k_y y)}\, dx\, dy. \end{aligned} \tag{5}$$

Taking the transform of (4) yields

$$\tilde{p}_\phi(\kappa) = \frac{ik^2}{2}\frac{e^{i\gamma L}}{\gamma}[\tilde{F}(\alpha, \beta) + 2\sin\phi\,\tilde{u}(\alpha, \beta) - 2\cos\phi\,\tilde{v}(\alpha, \beta)] \tag{6}$$

where

$$\begin{aligned} &|\kappa| \leqslant k \\ &\gamma = \sqrt{k^2 - \kappa^2} \\ &\alpha = \kappa\cos\phi + (k - \gamma)\sin\phi \\ &\beta = \kappa\sin\phi + (\gamma - k)\cos\phi. \end{aligned} \tag{7}$$

Note that the pressure transform depends not only on the scattering function but also each component of velocity. The relative contribution from each velocity component depends explicitly on the view angle. The restriction $|\kappa| \leqslant k$ can be interepreted as ignoring the

evanescent component of the scattered field. Equation (6) is derived by using an integral form of the Hankel function [10]

$$H_0^{(1)}(kR) = \pi^{-1} \int_{-\infty}^{\infty} \gamma^{-1} \exp[\mathrm{i}[\kappa(\xi - \xi') + \gamma(L - \eta')]] \, \mathrm{d}\kappa. \tag{8}$$

For convenience, define the filtered scattered field as

$$\tilde{D}_\phi(\kappa) = \frac{-\mathrm{i}\gamma}{2k^2} \mathrm{e}^{-\mathrm{i}\gamma L} \tilde{p}_\phi(\kappa). \tag{9}$$

Consider the scattered field measured from direction $\phi + \pi$. If the medium is lossless, the scattering function and the velocity are real functions. The associated transforms will display a conjugate symmetry [11], e.g. $\tilde{F}(\alpha, \beta) = \tilde{F}^*(-\alpha, -\beta)$. From (6)–(9),

$$\tilde{D}^*_{\phi+\pi}(\kappa) = [\tilde{F}(\alpha, \beta) - 2\sin\phi\tilde{u}(\alpha, \beta) + 2\cos\phi\tilde{v}(\alpha, \beta)]. \tag{10}$$

Taking the average of the filtered pressure data from opposing views yields

$$\begin{aligned} \tilde{\sigma}_\phi(\kappa) &\equiv \tfrac{1}{2}[\tilde{D}_\phi(\kappa) + \tilde{D}^*_{\phi+\pi}(\kappa)] \\ &= \tilde{F}(\alpha, \beta). \end{aligned} \tag{11}$$

Equation (11) shows that by appropriately combining data from opposing views the effects of the fluid motion can be removed. It is well known that if a simple ray model is used in the forward scattering problem, the measured time-of-flight data from opposing views are simply averaged to remove the first order effects of motion [1]. For the wave equation approach taken here, the measured data from each view are a coherent (complex) pressure field and the more complicated processing implied by (9)–(11) is required.

The known $\tilde{\sigma}_\phi(\kappa)$ maps onto a semicircle of radius $k$ in the Fourier space of $\tilde{F}$ (figure 2). This type of mapping between the measured data and the unknown was first derived by Wolf [12]. By making measurements over a continuum of view angles, Fourier space is effectively 'filled' out to a radius of $\sqrt{2}k$. The inverse transform of this data is then interpreted as a low-pass filtered version of the true scattering function. Physically, the reconstruction is low-pass filtered because details of the medium significantly smaller than the wavelength of the probing wave cannot be recovered. Assuming a stationary medium, Devaney [6] showed how to combine the measurements in a filtered backpropagation reconstruction algorithm. Equation (11) suggests that by first preprocessing the data by combining opposing views, a similar reconstruction algorithm for the scattering function could be derived for a moving medium. The development closely parallels Devaney's derivation and is omitted here for brevity.

Averaging opposing views removed the influence of the velocity and allowed the scattering function to be reconstructed. Taking the difference between opposing views,

$$\begin{aligned} \tilde{\Delta}_\phi(\kappa) &\equiv \tfrac{1}{4}\mathrm{i}[\tilde{D}_\phi(\kappa) - \tilde{D}^*_{\phi+\pi}(\kappa)] \\ &= \mathrm{i}\sin\phi\tilde{u}(\alpha, \beta) - \mathrm{i}\cos\phi\tilde{v}(\alpha, \beta) \end{aligned} \tag{12}$$

removes the effect of the scattering function. The known $\tilde{\Delta}_\phi(\kappa)$ is a linear combination of the unknowns $\tilde{u}$ and $\tilde{v}$ taken along semicircles in their respective Fourier spaces. The objective is to separate these two contributions and reconstruct the individual components

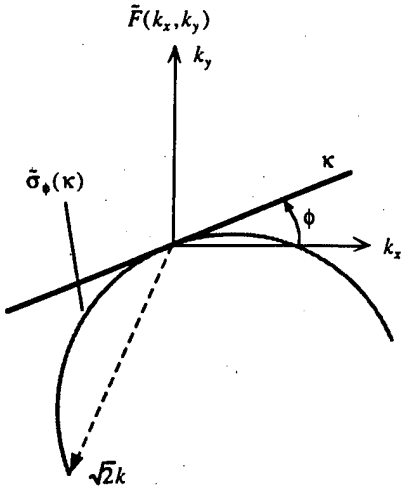


**Figure 2.** Fourier domain mapping for the scattering function $F$. The measured scattered fields from opposing directions are Fourier transformed, filtered and appropriately combined to yield $\tilde{\sigma}_\phi(\kappa)$. This function maps onto a semicircle in the Fourier space of $F$.

of the vector velocity. To accomplish this separation, a second relationship between $\tilde{u}(\alpha, \beta)$ and $\tilde{v}(\alpha, \beta)$ is required.

For the special case of a divergence free flow, the isolation of the two velocity components is easily achieved. In Fourier space, a divergence free flow satisfies

$$\alpha\tilde{u}(\alpha, \beta) + \beta\tilde{v}(\alpha, \beta) = 0. \tag{13}$$

Taken together, (12) and (13) constitute two equations for the two unknown velocity components.

The reconstruction becomes more complicated if it is not known *a priori* that the flow is divergence free. Assuming a straight-ray acoustics model, Norton [2] showed for this more general case that the two velocity components could not be isolated; vector inversion for this forward model is an underdetermined problem. We now show that by using the wave-based forward scattering model in (4), the inversion can be performed.

Consider any point $(\alpha, \beta)$ in the Fourier spaces of $\tilde{u}$ and $\tilde{v}$ where $0 < \alpha^2 + \beta^2 < 2k^2$. It is clear that two data arcs will pass through this point (figure 3). Let $\kappa = k\cos\chi$. It can be shown that

$$\begin{aligned}\tilde{\Delta}_\phi(k\cos\chi) &= \mathrm{i}\sin\phi\tilde{u}(\alpha, \beta) - \mathrm{i}\cos\phi\tilde{v}(\alpha, \beta)\\ \tilde{\Delta}_\theta(-k\cos\chi) &= \mathrm{i}\cos(\phi + \chi)\tilde{u}(\alpha, \beta) + \mathrm{i}\sin(\phi + \chi)\tilde{v}(\alpha, \beta)\end{aligned} \tag{14}$$

where

$$\theta = \phi + \chi + \pi/2. \tag{15}$$

Using (7), the point $(\alpha, \beta)$ can be written in terms of the two angles

$$\begin{aligned}\alpha &= k\sin\phi + k\cos(\phi + \chi)\\ \beta &= -k\cos\phi + k\sin(\phi + \chi).\end{aligned} \tag{16}$$

The system of equations in (14) can be solved except when $\chi = \pi/2$. From figure 3, this corresponds in frequency to $\alpha = \beta = 0$, or, in the spatial domain, to the mean value of the flow that is taken to be zero. Solving (14) yields

$$\begin{bmatrix} \tilde{u}(\alpha, \beta) \\ \tilde{v}(\alpha, \beta) \end{bmatrix} = \frac{-\mathrm{i}}{\cos\chi} \begin{bmatrix} \sin(\phi + \chi) & \cos\phi \\ -\cos(\phi + \chi) & \sin\phi \end{bmatrix} \begin{bmatrix} \tilde{\Delta}_\phi(k\cos\chi) \\ \tilde{\Delta}_\theta(-k\cos\chi) \end{bmatrix}. \tag{17}$$

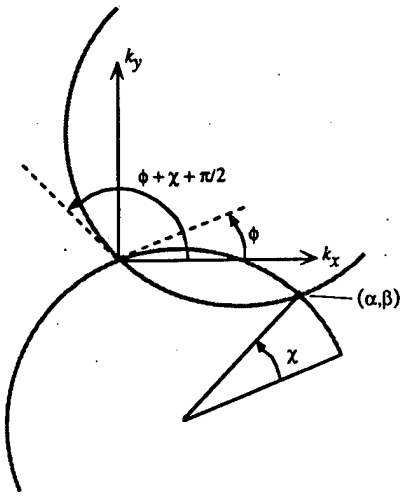


**Figure 3.** Fourier domain mapping for the vector velocity components. Data from experiments at view angles $\phi$ and $\phi + \chi + \pi/2$ intercept at point $(\alpha, \beta)$.

Equation (17) is a distinctly finite wavelength result. To show this, note that the radii of the semicircles in figure 3 are equal to $k$ and hence would increase linearly with frequency. In the high frequency limit, the two semicircles approach straight lines that can then intercept only at the origin. Consequently, a forward model that assumed an infinite frequency, i.e. ray theory, would not be able to separate the two components of velocity; this is consistent with Norton's result [2].

Equation (17) also suggests that there is not a simple one-to-one mapping between the measured data at a single view and the unknown functions. To recover a particular point $(\alpha, \beta)$, the processed data $\tilde{\Delta}$ must be used from two angles. From (12), each $\tilde{\Delta}$ in turn depends on measurements made from opposing directions. Hence to isolate a single point in the Fourier space of either velocity component, data from four views must be appropriately processed and combined. The process of combining various views and generating a reconstruction can be implemented in a filtered backpropagation algorithm.

## 3. Filtered backpropagation algorithm for vector velocity

A tomographic reconstruction algorithm is directly tied to the assumed transmission model for the forward problem. If the data are assumed to be simple projections of the unknown, the reconstruction is often generated by filtered backprojection. The measured projections from each view are first filtered and then backprojected along straight ray paths throughout

the image space. Superimposing the individual images yields the reconstruction. If the measured data are assumed to satisfy a wave equation, backprojection must be replaced by backpropagation. In backpropagation, the measured data are propagated through the image space using a range-dependent propagation kernel that compensates for diffraction in the forward problem. Devaney derived the original filtered backpropagation algorithm for reconstructing the scalar index of refraction for a stationary medium [6].

In this section, a filtered backpropagation algorithm for the vector velocity is derived. Following Devaney, we assume the measured data from each view are continuous and noise free and that the medium can be probed over a continuum of view directions. The result is a closed form inversion that is exact to within the assumed forward scattering model and that can be compared to the stationary medium result.

The low-pass filtered version of the $x$-component of velocity is defined by

$$u_{\mathrm{lp}}(x, y) = \frac{1}{4\pi^2} \int\int_{\mathfrak{R}} \tilde{u}(\alpha, \beta) e^{i(\alpha x + \beta y)} \, d\alpha \, d\beta \tag{18}$$

where $\mathfrak{R} : 0 < \alpha^2 + \beta^2 < 2k^2$. The variables of integration are changed to the angles $\phi$ and $\chi$. Calculating the Jacobian from (16) yields

$$d\alpha \, d\beta = k^2 |\cos \chi| d\phi \, d\chi \tag{19}$$

and (18) becomes

$$u_{\mathrm{lp}}(x, y) = \frac{k^2}{4\pi^2} \int_0^{2\pi} d\phi \int_0^{\pi/2} d\chi \, \cos(\chi) \tilde{u}(\alpha, \beta) e^{i(\alpha x + \beta y)} \tag{20}$$

where the limits on the $\chi$ integration allow the absolute value from the Jacobian to be dropped. Using the expression for $\tilde{u}(\alpha, \beta)$ from (17) yields

$$u_{\mathrm{lp}}(x, y) \equiv u^{(1)} + u^{(2)} \tag{21}$$

where

$$u^{(1)} = \frac{-ik^2}{4\pi^2} \int_0^{2\pi} d\phi \int_0^{\pi/2} d\chi \, \sin(\phi + \chi) \tilde{\Delta}_\phi(k \cos \chi) e^{i(\alpha x + \beta y)} \tag{22}$$

$$u^{(2)} = \frac{-ik^2}{4\pi^2} \int_0^{2\pi} d\phi \int_0^{\pi/2} d\chi \, \cos(\phi) \tilde{\Delta}_\theta(-k \cos \chi) e^{i(\alpha x + \beta y)}. \tag{23}$$

Equation (23) is rewritten in two steps. First, re-order the integrations and change variables from $\phi$ to $\theta$ via (15):

$$u^{(2)} = \frac{-ik^2}{4\pi^2} \int_0^{\pi/2} d\chi \int_{\chi+\pi/2}^{\chi+5\pi/2} d\theta \, \sin(\theta - \chi) \tilde{\Delta}_\theta(-k \cos \chi) e^{i(\alpha x + \beta y)} \tag{24}$$

where $\alpha$ and $\beta$ from (16) are expressed in the new variables. Since the integrand is periodic in $\theta$ with period $2\pi$, the limits can be changed to $[0, 2\pi)$. Again reordering the integrations and letting $\chi' = \pi - \chi$ yields

$$u^{(2)} = \frac{ik^2}{4\pi^2} \int_0^{2\pi} d\theta \int_{\pi/2}^{\pi} d\chi' \, \sin(\theta + \chi') \tilde{\Delta}_\theta(k \cos \chi') e^{i(\alpha x + \beta y)} \tag{25}$$

where $\alpha$ and $\beta$ are again expressed in the new variables. Comparing (22) and (25) shows that they differ only in sign and on the limits of integration. Recombining via (21) gives finally

$$u_{lp}(x, y) = \frac{-ik^2}{4\pi^2} \int_0^{2\pi} d\phi \int_0^{\pi} d\chi \, \frac{|\cos\chi|}{\cos\chi} \sin(\phi + \chi) \tilde{\Delta}_\phi(k\cos\chi) e^{i(\alpha x + \beta y)}. \tag{26}$$

A similar development for the $y$-component of velocity gives

$$v_{lp}(x, y) = \frac{ik^2}{4\pi^2} \int_0^{2\pi} d\phi \int_0^{\pi} d\chi \, \frac{|\cos\chi|}{\cos\chi} \cos(\phi + \chi) \tilde{\Delta}_\phi(k\cos\chi) e^{i(\alpha x + \beta y)}. \tag{27}$$

Both low-pass reconstructions are real functions. To simplify the development, define the complex combination of the two reconstructions as

$$Z(x, y) = u_{lp}(x, y) + iv_{lp}(x, y). \tag{28}$$

By taking the real and imaginary parts of $Z(x, y)$, low-pass filtered versions of the velocity components $u(x, y)$ and $v(x, y)$ are extracted, respectively. Returning to the original variable $\kappa = k\cos\chi$ and combining (26)–(28) yields

$$Z(x, y) = \frac{-k}{4\pi^2} \int_0^{2\pi} d\phi \, e^{i\phi} \int_{-k}^{k} d\kappa \, \gamma^{-1} \operatorname{sgn}(\kappa)(\kappa + i\gamma) \tilde{\Delta}_\phi(\kappa) e^{i(\alpha x + \beta y)} \tag{29}$$

where sgn is the sign function [11] taking values +1 for $\kappa > 0$ and −1 for $\kappa < 0$.

Two observations can be made from (29). First, the integrand depends on $\tilde{\Delta}$ at the single view angle $\phi$. The explicit combination of data at view angles $\phi$ and $\theta$ suggested by (21) has been built implicitly into the reconstruction algorithm. Second, the result is similar in form to the standard filtered backpropagation algorithm: data from the various views are filtered, backpropagated and combined by integrating over $\phi$. In contrast to the standard result, however, here the various views are phase shifted by the factor $e^{i\phi}$. The need for this bias is suggested by the forward problem. For a given view angle, only those components of velocity tangential to the incident plane wave, i.e. $\hat{\eta} \cdot (u\hat{x} + v\hat{y})$, contribute to the scattered field. The bias in the inversion compensates for the bias in the forward problem.

From (12), $\tilde{\Delta}_\phi(\kappa)$ is a filtered combination of the scattered field data taken from opposing views. This preprocessing step effectively removes the contribution from the scalar index of refraction on the scattered field. Since in some practical applications this contribution can be an order of magnitude greater than that from the vector velocity [13, 14], its explicit cancellation may be desirable for stability in the inversion. For the ideal noise free case considered here, preprocessing is not required and an inversion algorithm can operate directly on the measured pressure. A convolutional backpropagation algorithm is now derived that operates in the spatial domain on the untransformed data. Substituting (9) and (12) into (29) gives

$$Z(x, y) = Z^{(1)} + Z^{(2)} \tag{30}$$

where

$$Z^{(1)} = \frac{-1}{8k\pi^2} \int_0^{2\pi} d\phi \, e^{i\phi} \int_{-k}^{k} d\kappa \, \operatorname{sgn}(\kappa)(\kappa + i\gamma) \tilde{p}_\phi(\kappa) e^{-i\gamma L} e^{i(\alpha x + \beta y)} \tag{31}$$

$$Z^{(2)} = \frac{-1}{8k\pi^2} \int_0^{2\pi} d\phi \, e^{i\phi} \int_{-k}^{k} d\kappa \, \operatorname{sgn}(\kappa)(\kappa + i\gamma) \tilde{p}^*_{\phi+\pi}(\kappa) e^{+i\gamma L} e^{i(\alpha x + \beta y)}. \tag{32}$$

In (32), let $\phi' = \phi + \pi$. Exploiting the periodicity of the integrand to change the limits and returning to the original dummy variable yields

$$Z^{(2)} = \frac{+1}{8k\pi^2} \int_0^{2\pi} d\phi\, e^{i\phi} \int_{-k}^{k} d\kappa\ \mathrm{sgn}(\kappa)(\kappa + i\gamma)\tilde{p}_\phi^*(\kappa)e^{+i\gamma L}e^{-i(\alpha x+\beta y)}. \quad (33)$$

Using figure 1, the reconstruction point $(x, y)$ can be expressed in the rotated coordinates $(\xi, \eta)$. Combining with $\alpha$ and $\beta$ from (7) gives

$$\alpha x + \beta y = \kappa\xi + (\gamma - k)\eta. \quad (34)$$

Make the final change of variables $\kappa \to -\kappa$ in (33). Then using (34) and recombining $Z^{(1)}$ and $Z^{(2)}$ using (30) yields

$$Z(x, y) = \frac{-1}{8k\pi^2} \int_0^{2\pi} d\phi\, e^{i\phi} \int_{-\infty}^{\infty} d\kappa\, [\tilde{p}_\phi(\kappa)\tilde{G}^*(\kappa, \eta) - \tilde{p}_\phi^*(-\kappa)\tilde{G}(\kappa, \eta)]e^{i\kappa\xi} \quad (35)$$

where

$$\tilde{G}(\kappa, \eta) = \begin{cases} \mathrm{sgn}(\kappa)(\kappa + i\gamma)e^{ik\eta}e^{i\gamma(\eta-L)} & |\kappa| < k \\ 0 & |\kappa| \geqslant k. \end{cases} \quad (36)$$

Equation (35) gives the reconstruction as the inverse transform of the difference between two products. This can be rewritten in terms of the untransformed data using the convolution theorem [11]:

$$Z(x, y) = \frac{-1}{4k\pi} \int_0^{2\pi} d\phi\, e^{i\phi} \int_{-\infty}^{\infty} d\xi'\, [p_\phi(\xi')G^*(\xi' - \xi, \eta) - p_\phi^*(\xi')G(\xi - \xi', \eta)] \quad (37)$$

where the backpropagation kernel is given by the inverse transform

$$G(\xi, \eta) = \frac{1}{2\pi} \int_{-\infty}^{\infty} \tilde{G}(\kappa, \eta)e^{i\kappa\xi}\, d\kappa. \quad (38)$$

The reconstruction algorithm can be summarized as follows. For a particular view direction $\phi$, the measured scattered field and its complex conjugate are convolved with the backpropagation kernel and its complex conjugate as suggested by the inner integral in (37). The resulting complex image is then phase shifted by $e^{i\phi}$. The procedure is repeated for all view directions with the resulting images superimposed. By taking the real and imaginary parts of the combined image, low-pass filtered versions of the respective velocity components $u(x, y)$ and $v(x, y)$ are extracted (equation (28)).

## 4. Discussion

Characterizing a moving, inhomogeneous fluid from acoustic transmission measurements is an inverse problem with many practical applications. The approach used in the inversion is largely predicated on the assumed forward model for the acoustics. If a straight-ray transmission model is assumed, then inversion for the vector flow velocity is an underdetermined problem. The primary result of this paper is that a complete inversion for velocity is possible using a wave-based approach. The analysis establishes the information

content of coherent pressure measurements for weak scattering at a single frequency. A filtered backpropagation reconstruction algorithm has also been derived.

The inversion procedure is limited to two-dimensional geometries and assumes noiseless, continuous data measured over a continuum of view directions. The reconstructions are necessarily low-pass filtered versions of the original fields as details smaller than the ensonifying wavelength cannot be recovered. With these caveats, the inversions are unique and exact to within the validity of the Born approximation and the assumed forward scattering model in (1). Criteria for the validity of the Born approximation are well established and generally satisfied when the magnitude of the inhomogeneities is small compared to the background sound speed [9]. In deriving (1), terms involving spatial derivatives of the velocity are presumed small and have been neglected. The contribution to scattering from the neglected terms could become significant at spatial scales comparable to the wavelength. Neglecting these terms in the forward scattering model may impose a theoretical limitation on the inversion.

In a practical experiment, the flow could be probed from only a finite number of directions. Measurement noise and three-dimensional effects could be significant. The accuracy of the reconstruction would depend on the quality and quantity of the measurements, and on how the inversion algorithm was implemented. Consequently, the accuracy of a reconstruction is strongly dependent on the application. A study of these factors is beyond the intended scope of this paper. The presented analysis is not intended to model a specific physical situation or experiment, but rather to illustrate the advantages of diffraction tomography in as simple a setting as possible.

Various generalizations of this work can be contemplated. A wave-based approach makes possible the use of broad band ensonification. Often there is a duality between probing a medium from many directions using a single frequency and probing from a limited number of directions using a broad band pulse. Extensions to three dimensions and curved recording surfaces should also be possible. A further improved forward model that retained some of the terms neglected in (1) is also desirable.

## Acknowledgments

This research was sponsored by the Department of the Navy, Office of the Chief of Naval Research under Grant N00014-90-J-1369. This article does not necessarily reflect the position or the policy of the US Government, and no official endorsement should be inferred. It was conducted as part of the APL-UW Multiple Discipline Group research program.

## References

[1] Johnson S A, Greenleaf J F, Tanaka M and Flandro G 1977 Reconstructing three-dimensional temperature and fluid velocity vector fields from acoustic transmission measurements *ISA Trans.* **16** 3–15

[2] Norton S J 1988 Tomographic reconstruction of two-dimensional vector fields: Application to flow imaging *Geophys. J. R. Astron. Soc.* **97** 162–8

[3] Winters K B and Rouseff D 1990 A filtered backprojection method for the tomographic reconstruction of fluid vorticity *Inverse Problems* **6** L33–8

[4] Winters K B and Rouseff D 1993 Tomographic reconstruction of stratified fluid flow *IEEE Trans. Ultrason. Ferroelec. Freq. Control* **40** 26–33

[5] Mueller R K, Kaveh H and Iverson R D 1979 Reconstructive tomography and applications to ultrasonics *Proc. IEEE* **67** 567–87

[6] Devaney A J 1982 A filtered backpropagation algorithm for diffraction tomography *Ultrason. Imag.* **4** 336–50

[7] Morse P M and Ingard K U 1968 *Theoretical Acoustics* (New York: McGraw-Hill)
[8] Norton S J 1991 Reconstructing stratified fluid flow from reciprocal scattering measurements *J. Acoust. Soc. Am.* **89** 2567–72
[9] Ishimaru A 1978 *Wave Propagation and Scattering in Random Media* (New York: Academic)
[10] Morse P M and Feshbach H 1953 *Methods of Theoretical Physics* (New York: McGraw-Hill) p 823
[11] Bracewell R N 1986 *The Fourier Transform and Its Applications* 2nd edn (New York: McGraw-Hill)
[12] Wolf E 1969 Three-dimensional structure determination of semi-transparent objects from holographic data *Opt. Commun.* **1** 153–6
[13] Howe B M, Worcester P F and Spindel R C 1987 Ocean acoustic tomography: mesoscale velocity *J. Geophys. Res.* **92** 3785–805
[14] Rouseff D, Winters K B and Ewart T E 1993 Reconstruction of small-scale flow dynamics by acoustical tomography *Proc. OCEANS 93* **2** 408–12